

Preparation of a low proton resistance PBI/PTFE composite membrane

Hsiu-Li Lin^{a,b}, T. Leon Yu^{a,b,*}, Wei-Kai Chang^a,
Chien-Pang Cheng^a, Chih-Ren Hu^a, Guo-Bin Jung^b

^a Department of Chemical Engineering & Materials Science, Yuan Ze University, Chung-Li, Taoyuan 32003, Taiwan

^b Fuel Cell Center, Yuan Ze University, Chung-Li, Taoyuan 32003, Taiwan

Received 5 September 2006; received in revised form 15 November 2006; accepted 17 November 2006

Available online 22 December 2006

Abstract

We present a method for fabrication of poly(benzimidazole)/porous poly(tetra fluorocarbon) (PTFE) composite membranes. A coupling agent containing perfluorocarbon sulfonic acid ionomer is used as an interface between PTFE and poly(benzimidazole) (PBI), which contained –NH groups. The porous PTFE substrate was impregnated with a diluted PFSI coupling agent solution. The optimum concentration of the coupling agent solution was that the concentration of coupling agent was just high enough to cover the surface of the fibers of the porous PTFE substrate membranes. The PBI solutions were then fabricated onto the PTFE membranes containing the coupling agent to prepare the proton exchange composite membranes. The PBI/PTFE composite membrane had a film thickness of $\sim 22 \mu\text{m}$ and thus a lower proton resistance than a PBI membrane with a film thickness of $\sim 100 \mu\text{m}$. The PEMFC single cell tests showed that PBI/PTFE composite membrane had a better performance than PBI.

© 2006 Elsevier B.V. All rights reserved.

Keywords: Poly(benzimidazole); PTFE; Composite membranes; Fuel cell

1. Introduction

It is generally accepted that polymer electrolyte membrane fuel cell (PEMFC) presents an attractive alternative to traditional power sources, due to high efficiency and low-pollution. In a PEMFC, the proton-conducting membrane is located between the cathode and anode and transports protons formed near the catalyst at the hydrogen electrode to the oxygen electrode thereby allowing external current to be drawn from the cell. The membranes for high performance PEM fuel cells have to meet the following requirements [1]: (1) low cost material; (2) high proton conductivity; (3) good water uptake; (4) low gas permeability; (5) reliable durability. Nafion (trade name of the DuPont Co) membrane is a successful proton exchange membrane (PEM) and a fast proton-conducting separator in the PEMFC, which has been proven to have excellent perfor-

mance at temperatures below 90°C using hydrogen as fuel [2]. However, the requirement of high humidity for its sulfonated side chains to conduct protons, causes problems in PEMFC operations at temperatures higher than 90°C , due to the high evaporation of water and low humidity of Nafion membranes. Although it had been reported that a Nafion-based PEMFC showed good performance while operating at $120\text{--}150^\circ\text{C}$ with a humidifier to raise the humidity of the membrane ($>50\%$ relative humidity), it is impractical from a system point of view to operate the fuel cell with a humidifier, which causes a complex system design [3].

In the past decade, researchers [4–10] have made efforts to develop hydrocarbon membranes for PEMFCs working at high temperatures ($100^\circ\text{C} < \text{Temp} < 200^\circ\text{C}$). One of the most prominent membranes is PBI (polybenzimidazole) doped with phosphoric acid [5], in which phosphoric acid acts as the proton-conducting carrier and no water is needed for proton conduction in the membranes. Thus PEMFCs using PBI doped with phosphoric acid as the proton-conducting separators are available to work at high temperatures ($100^\circ\text{C} < \text{Temp} < 200^\circ\text{C}$) in a low humidity environment [5,9,10]. The advantages of high temperature working PEMFCs are [2]: (1) lower CO adsorption on

* Corresponding author at: Department of Chemical Engineering & Materials Science, Yuan Ze University, Nei-Li, Chung-Li, Taoyuan 32003, Taiwan.
Tel.: +886 3 4638800x2553; fax: +886 3 4559373.

E-mail address: cetlyu@saturn.yzu.edu.tw (T.L. Yu).

the catalysts leading to lower CO poisoning of catalysts, thus a higher efficiency of catalysts; (2) lower heat exchange area needed to dissipate excess heat; (3) the electrochemical reaction product, i.e. water, is easier to be evaporated at higher temperatures, thus easier water management. The lower CO adsorption on the catalyst at higher temperatures leads a fuel cell easier to be operated with a liquid fuel reformer, which for kinetic reasons is run at a high temperature, yielding a significant amount of CO. The lower heat exchange area and easier water management results in a simpler design for such fuel cell systems.

The high cost of the cell components is the main impediment to the commercialization of PEMFCs. One of the primary contributors to the PEM fuel cell's high cost is the Nafion and PBI membrane. Recent research reports have shown that cost reduction can be realized by replacing the Nafion membrane by a poly(tetrafluoroethylene) (PTFE)-based composite membrane [11–23]. Composite membranes may be prepared by impregnation of a low cost microporous supporting material, i.e. porous PTFE, with a Nafion solution. It is important to note that the composite membranes contain much less expensive Nafion resin than the commercial Nafion membranes, such as Nafion-117 (in thickness of 175 μm), Nafion-115 (in thickness of 125 μm), and Nafion-112 (in thickness of 50 μm), thus the cost of composite membranes is much lower than that of the commercial PFSI membranes.

In this paper, we report the preparation of a PBI/PTFE composite membrane. Perfluorosulfonic acid ionomer (PFSI) was used as a coupling agent of PTFE and poly(benzimidazole) (PBI), which contained $-\text{NH}$ groups. The porous PTFE substrate was impregnated with a diluted PFSI coupling agent solution. The optimum concentration of the coupling agent solution is that the concentration of coupling agent is just high enough to cover the surface of the fibers of porous the PTFE substrate membranes. The PBI solutions were then fabricated onto the PTFE membranes containing the coupling agent to prepare the proton exchange composite membranes. The PBI/PTFE composite membrane had a film thickness of 20–22 μm and thus a lower proton resistance than a PBI membrane with a film thickness of 80–100 μm . PFSI is comprised of a perfluorocarbon main chain, which is compatible with porous PTFE, and ether fluorocarbon sulfonic acid side chains, which is compatible with $-\text{NH}$ groups of PBI. Thus a good bonding interface between the porous PTFE and PBI can be obtained. Because of the higher mechanical strength of PTFE compared with PBI, for fuel cells applications, the thickness of PBI/PTFE composite membranes can be lower than that of PBI membranes. The PEMFC single cell tests showed that PBI/PTFE composite membranes had a better performance than pure PBI membranes, because of the thinness of PBI/PTFE composite membranes and thus lower proton resistance of proton exchange membranes.

2. Experimental

2.1. Materials

PBI was synthesized from 3,3'-diamino benzidine (Aldrich Chemical Co.) and isophthalic acid (Aldrich Chemical Co.)

using polyphosphoric acid (Aldrich Chemical Co.) as a solvent. The detailed polymerization procedures were same as those reported by Ueda et al. [24]. The inherent viscosity (I.V.) was measured by dissolving 0.5 wt% of PBI in 98 wt% sulfuric acid solution using an Ubbelohde viscometer (with a water flow time of 98 s) and an I.V. of 1.52 dL/g was obtained, which corresponded to $M_v = 1.0 \times 10^5$ g/mol calculated using an equation derived by Choe and Choe [25]. A porous PTFE membrane (Yue-Ming-Tai Chemical Ind. Co., Taiwan) with a thickness of 16 ± 2 μm , pore sizes of 0.5 ± 0.1 μm , and porosity of $85 \pm 5\%$ was used as a supporting material of composite membranes. A 5 wt% PFSI solution (EW = 1100, Du Pont Co.) was used as a coupling agent. The solvent mixture of the PFSI solution water, propanol, ethanol, methanol and unspecified mixed ethers [26].

2.2. Preparation of PBI membranes

PBI/LiCl/DMAc (2 wt%) (*N,N'*-dimethyl acetamide) solution was prepared by dissolving 10 g PBI and 15 g LiCl in 500 ml DMAc under a nitrogen atmosphere at 150 °C. The DMAc solvent was then evaporated from the solution at 80 °C under vacuum to obtain a solution with a PBI content of around 8 wt%. The PBI solution was coated on a glass plate using a film applicator with a gate thickness of 130 μm . The glass plate with a thin film of PBI solution was heated at 80 °C for 1 h and then 120 °C for 5 h under vacuum to remove DMAc solvent. The PBI membrane was then immersed in distilled water for 3 days and the water was changed each day to remove LiCl. Finally, the PBI membrane was immersed in 85 wt% phosphoric acid solution for 3 days. The final thickness of PBI membrane was around ~ 100 μm .

2.3. Preparation of PBI/PTFE composite membranes

(a) The solvent of as received PFSI solution was evaporated under vacuum at 60 °C and the residual solid PFSI resin was mixed with 2-propanol/water (4/1 wt ratio) mixture solvent to a solution containing 0.7 wt% of PFSI. Porous PTFE membrane was mounted on a 12 cm \times 12 cm steel frames and boiled in acetone at 55 °C for 1 h. This pre-treated PTFE membrane was then impregnated with a 0.7 wt% PFSI solution for 24 h. These impregnated membranes were then annealed at 130 °C for 1 h. After annealing, the membrane was then swollen with distilled water for 24 h. Thus the porous PTFE membrane was coated with a thin film of PFSI. (b) The porous PTFE membrane coated with a thin film of PFSI was impregnated in a PBI/LiCl/DMAc (4.5/4.5/100 in wt ratio) solution for 5 min, the membrane was then heated at 80 °C for 30 min and then 120 °C for 30 min under vacuum. The process of membrane impregnation in PBI/LiCl/DMAc solution and annealing was repeated for three to five times to obtain a composite membrane with a desired film thickness. The PBI/PTFE composite membrane was then immersed in distilled water for 3 days and the water was changed each day to remove LiCl. Finally, the PBI/PTFE composite membrane was immersed in 85 wt% phosphoric acid for 3 days. Table 1 lists the final compositions and film thickness of PBI/PTFE composite membranes and PBI membrane.

Table 1
Compositions and film thickness of dried membranes

Membrane	PBI (wt%)	PTFE (wt%)	Coupling agent (wt%)	Phosphoric acid (wt%)	Thickness (μm)
PBI/PTFE-2	39.0	18.7	4.3	38.0	22 \pm 3
PBI/PTFE-1	36.2	24.2	5.5	33.1	19 \pm 2
PBI/PTFE-0	20.7	79.3	–	–	17 \pm 2
PBI	100.0	–	–	–	100 \pm 3

2.4. Characterizations of PBI membrane and PBI/PTFE composite membranes

The morphology of membranes was studied using a scanning electron microscope (SEM, model JSM-5600, Jeol Co., Japan). The sample surface was coated with gold powder under vacuum before SEM observation was performed. Thermal stability of membranes was investigated, using a thermogravimetric analyzer (TGA, TA model Pyris-1), with sample sizes of 6–10 mg, and a heating rate of 10 K/min and a nitrogen flow rate of 10 ml/min. The mechanical property of membranes was tested, using an Instron testing machine (model 4204), in accordance with JIS-K7127. The membrane acid-doping contents were determined by weighing the membranes before and after doping phosphoric acid. In order to avoid the deviation from moisture contents, before weighing, the membranes were dried by evaporating the water at 110 °C under vacuum for more than 10 h until an unchanged weight was obtained.

The ionic conductivities (σ) of membranes were measured by using a four-probe cell similar to the design reported by Hasiotis et al. [27]. The cell was introduced in a stainless still vessel that was immersed in an oil bath to control cell temperature. The measurements were performed at temperatures of 150 and 180 °C and a relative humidity of 18 \pm 2%. The membranes were strips with sizes of 4 cm \times 1 cm. Two platinum foils were used to apply current to the ends of the membrane while the other two platinum probe wires spaced 1 cm apart were employed to measure the potential drop along the film near the center of the membrane. A thermocouple was arranged near the sample for monitoring its temperature. The relative humidity was controlled by passing a mixture of humidified and dry nitrogen through the cell and was monitored using a hygrometer. Two flow meters were used to control the ratio of dry and humidified nitrogen that were mixed in a chamber placed just before the cell. The measurements were carried out by ac impedance spectroscopy using a Solartron 1260 gain phase analyzer interfaced to a Solartron 1480 multimeter.

Gas permeability of membranes was investigated using an apparatus designed by our lab. A device of holding a membrane was located between two vessels, with the volume of vessel-1 of 3000 ml and that of vessel-2 of 200 ml. At the beginning of gas permeability test, vessel-1 was filled with H₂ gas under a pressure of 294 kPa and vessel-2 was kept under vacuum. The membrane holder was kept at a temperature of 25 °C. The gas permeability of the membrane is characterized by measuring the pressure of vessel-2 (P_2) versus testing time. The variation of vessel-2 pressure P_2 against measuring time was recorded till P_2 reaching 2.94 kPa for each membrane. A membrane with

a higher gas permeability (or poor gas barrier) should have a higher P_2 increment rate dP_2/dt , i.e. a shorter time for P_2 to reach 2.94 kPa.

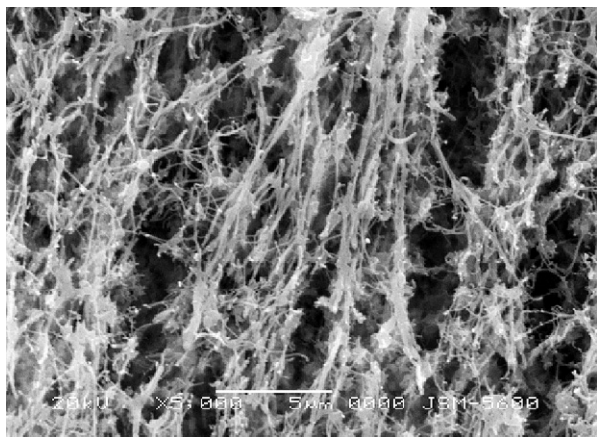
2.5. Fuel cell performance test

The PBI and PBI/PTFE composite membranes prepared in our lab were used to prepare membrane electrode assemblies (MEA). The catalyst was Pt–C (E-TEK, 20 wt% Pt) and the Pt loadings of anode and cathode were 0.5 mg/cm². Pt–C/PBI/LiCl/DMAc (3.5/1/0.3/49 by wt) catalyst solution was prepared by ultrasonic disturbing for 5 h. In catalyst ink solution, LiCl was a stabilizer of PBI/DMAc solution. The catalyst ink was brushed onto carbon cloth (E-TEK, HT 2500-W), dried at 110 °C in a conventional oven to calculate catalyst loading. The catalyst coated carbon cloths were immersed in deionized water for 24 h to remove LiCl. They were then doped with phosphoric acids by dipping in 5% H₃PO₄ solution for 24 h and dried in oven at 110 °C. The membrane was sandwiched between two carbon cloths coated with a catalyst layer and pressed at 150 °C with a pressure of 50 kg/cm² for 5 min to obtain a MEA. The performances of single cells were tested at 150 and 180 °C using a FC5100 fuel cell testing system (CHINO Inc., Japan). The area of testing fixture was 5 cm \times 5 cm and the anode H₂ cathode O₂ input flow rates were 300 ml/min. Both H₂ and O₂ flows were unhumidified.

3. Results and discussion

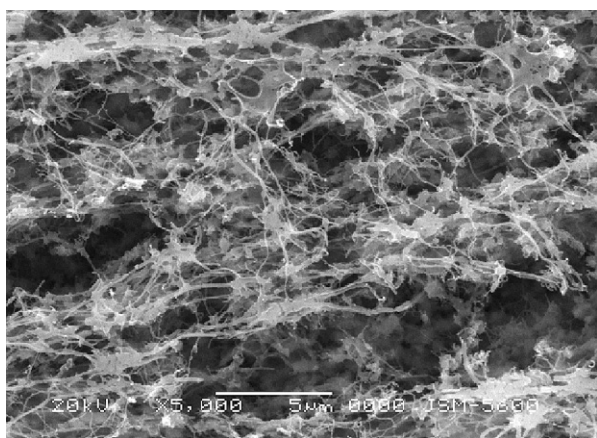
3.1. SEM study of composite membranes

Fig. 1 shows SEM micrograph of the surface of as received porous PTFE membrane. This micrograph shows that there are fibers with knots visible in the membrane and among the fibers and knots there are micro-pores in PTFE membranes. Fig. 2 shows the SEM micrograph of the surface of PBI/PTFE-0 composite membrane, which was prepared by impregnating porous PTFE with PBI/DMAc/LiCl solution without pre-treating with a PFSI solution. As shown in Fig. 2, the porous PTFE membrane impregnated with a PBI solution without pre-treating with a PFSI coupling solution had little PBI polymer coated on the surface of fibers and knots. The surface of the composite membranes had micro-pores and fiber-like structures are visible in the micrograph. This result suggests that PBI is not compatible with PTFE and the bonding between PBI and PTFE is weak. Fig. 3 shows the SEM micrograph of porous PTFE membrane after impregnated with a 0.7 wt% PFSI solution. A thin film of PFSI resin covered on the surface of fibers and knots of PTFE



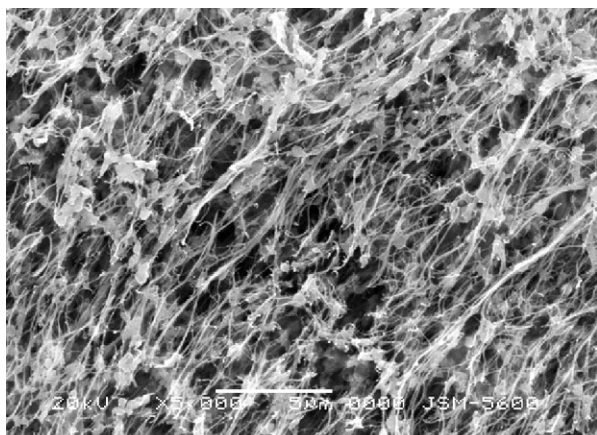
5 μm

Fig. 1. SEM micrograph (5000 \times) of porous PTFE membrane.



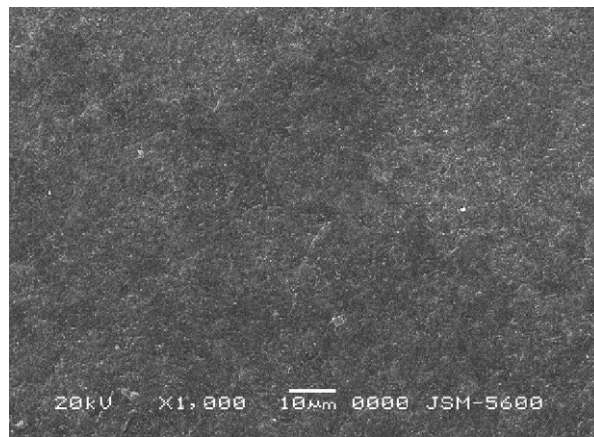
5 μm

Fig. 2. SEM micrograph of (5000 \times) of PBI/PTFE-0 composite membrane, which was prepared by impregnating porous PTFE with PBI/DMAc/LiCl solution without pre-treating with a PFSI coupling solution.



5 μm

Fig. 3. SEM micrograph (5000 \times) of porous PTFE membrane after treatment with a 0.7 wt% PFSI coupling solution.



10 μm

Fig. 4. SEM micrograph (5000 \times) of PBI/PTFE-1 (thickness 19 μm) composite membrane, which was prepared by impregnating porous PTFE in a 0.7 wt% PFSI coupling solution and then in a PBI/DMAc/LiCl solution.

is visible. Fig. 4 is the micrograph of PBI/PTFE-1 composite membrane (thickness \sim 19 μm), which was prepared by impregnating porous PTFE in a 0.7 wt% PFSI solution and then in a 4.5 wt% PBI/DMAc/LiCl solution, as described in Section 2. Fig. 4 shows that all the voids of PTFE membranes had been filled and completely covered with PBI. It is known that PFSI resin composes of perfluorocarbon ($-\text{CF}_2-\text{CF}_2-$) main chains, which are compatible with PTFE, and sulfonated ether fluorocarbon ($-\text{OCF}_2-\text{CF}_2(\text{CF}_3)-\text{OCF}_2-\text{CF}_2-\text{OSO}_3\text{H}$) side chains, which is compatible with PBI. The side chain $-\text{OSO}_3\text{H}$ group of PFSI may react with $=\text{NH}$ groups of PBI and forms ionic compound. Thus PFSI acted as a coupling agent of PBI and PTFE, and PBI was well bonded with PTFE after the surface of PTFE was treated with a thin film of PFSI resin.

3.2. Gas permeability study

The H_2 gas permeability test of PBI/PTFE-1 (thickness 19 μm), PBI/PTFE-2 (22 μm), and PBI (thickness 100 μm) membranes were performed at 25 $^\circ\text{C}$. Fig. 5 shows the variation of vessel-2 pressure P_2 versus testing time. From Fig. 5, we found that P_2 value was almost \sim 0.0 kPa at the beginning of measurements. The vessel-2 pressure P_2 started to increase after t_{leak} . The t_{leak} indicates the “persistence time” for the membrane to against the gas pressure, and gas start to leak through the membrane after t_{leak} . The time t_{leak} and the time $t_{2.94\text{ kPa}}$, which is the time for P_2 to reach 2.94 kPa (\sim 3 kgf/cm 2), are listed in Table 2. The longer the t_{leak} and $t_{2.94\text{ kPa}}$ the better the gas barrier property of the membrane. These data show that t_{leak} and $t_{2.94\text{ kPa}}$ decreased in the sequence: PBI > PBI/PTFE-2 > PBI/PTFE-1, indicating PBI had the best gas barrier property in all of these membranes, because of its highest film thickness. However, the times “ $t_{\text{leak}} = 80\text{ h}$ ” “ $t_{2.94\text{ kPa}} = 118\text{ h}$ ” of PBI/PTFE-2 (thickness 22 μm) were close to those of PBI (thickness 100 μm), suggests that PFSI is a good coupling agent of PBI and PTFE

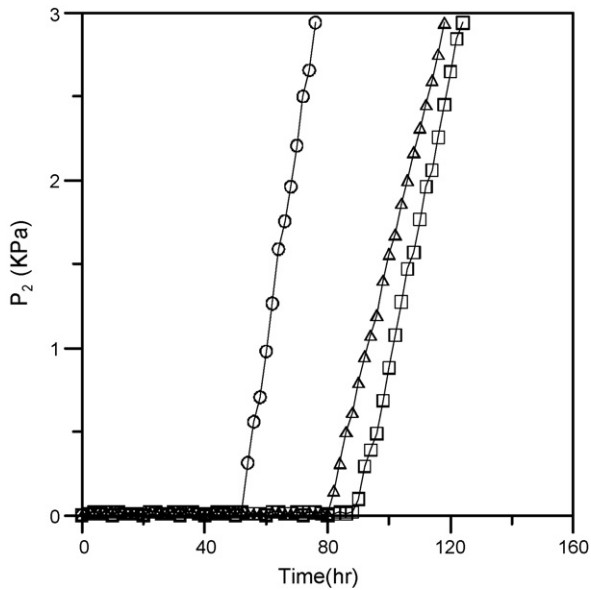


Fig. 5. Gas permeability tests of three membranes, vessel-2 pressure P_2 vs. testing time. Membranes: (□) PBI (100 μm); (○) PBI/PTFE-1 (19 μm); (△) PBI/PTFE-2 (22 μm).

and improves the bonding force between PBI and PTFE. It is known that PTFE has a strong mechanical strength and also a good barrier property for gas. The reinforcement of PBI with porous PTFE improved the mechanical strength (see Section 3.5) and barrier property of PBI, in spite of the lower thickness of PBI/PTFE than PBI.

3.3. Conductivity measurements

The conductivities of Nafion, PBI and PBI/PTFE composite membranes were measured using an ac impedance system at 150 and 180 °C with a relative humidity of $18 \pm 2\%$. The conductivity σ and the unit area resistance across the membrane thickness direction, $r = l/\sigma$ where l is the membrane thickness, of Nafion-117, PBI, and PBI/PTFE-2 are listed in Table 3. The data shown in Table 3 are the average values of three measurements and the standard deviations are around $\pm 5\%$. These data show that PBI and PBI/PFTE had higher conductivity than Nafion-117 at 150–180 °C. Though the conductivity of PBI/PTFE-2 composite membrane (22 μm) is lower than that of PBI (100 μm), however, due to the lower thickness of PBI/PTFE composite membrane, PBI/PTFE composite membrane has a lower resistance r than PBI membrane.

Table 2
Gas permeation measurements— t_{leak} and $t_{2.94 \text{ kPa}}$ data

Membrane	Thickness of membrane (μm)	t_{leak}^a (h)	$t_{2.94 \text{ kPa}}^b$ (h)
PBI	100.0	88	124
PBI/PTFE-1	19.0	52	76
PBI/PTFE-2	22.0	80	118

^a t_{leak} = the time for vessel-2 pressure P_2 starts to increase and larger than 0.0 kPa.

^b $t_{2.94 \text{ kPa}}$ = the time for vessel-2 pressure P_2 to reach 2.94 kPa.

Table 3

Conductivities σ and resistances per unit area r of membranes (relative humidity $18 \pm 2\%$)

	σ ($10^{-3} \text{ S cm}^{-1}$)	r ($\text{cm}^2 \text{ S}^{-1}$)
Nafion-117 ^a		
150 °C	1.03	5.42
180 °C	1.62	3.44
PBI ^a		
150 °C	14.4	0.183
180 °C	18.6	0.153
PBI/PTFE-2 ^a		
150 °C	4.76	0.133
180 °C	7.54	0.081

^a Membrane.

3.4. TGA analysis

Fig. 6 shows TGA heating scan curves of porous PTFE, PBI, PBI/PTFE-2 composite membrane containing 38.0 wt% of phosphoric acid, PBI/PTFE-2 composite membrane without doping with phosphoric acid. The weight loss at temperatures below 200 °C was due to the loss of moisture [curves (a–c)]. The data of Fig. 6 indicated thermal degradation temperature of PTFE was around 400–600 °C [curve (d)] and the thermal degradation of pure PBI was around 600–1200 °C [curve (a)]. The thermal decomposition of phosphoric acid in PBI had been investigated by Samms et al. [28] using thermogravimetric analysis in conjunction with mass spectrometry. According to Samms et al., the weight loss around 200–300 °C of PBI/PTFE-2 (containing 38.0 wt% phosphoric acid) [curve (b)] was due to the loss of water from the reaction of phosphoric acid to pyrophosphoric acid ($2\text{H}_3\text{PO}_4 \rightarrow \text{H}_4\text{P}_2\text{O}_7 + \text{H}_2\text{O}$) [28]. Above 600 °C additional weight loss of water of PBI/PTFE-2 (contain-

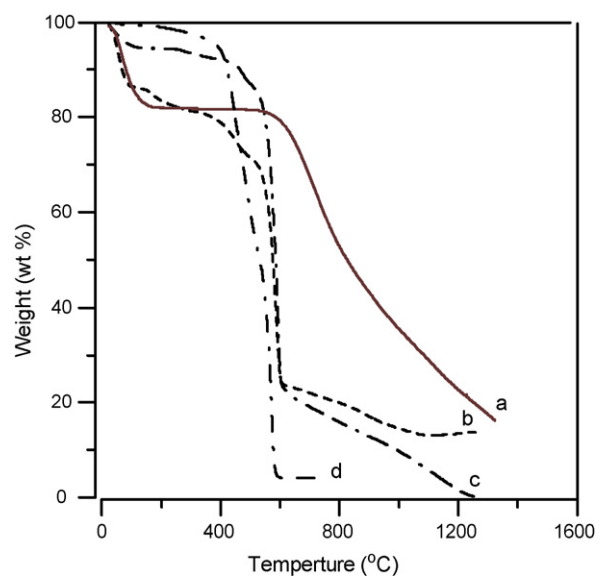


Fig. 6. TGA heating scan curves (scan rate 10 K/min, and N_2 flow rate 10 ml/min). (a) PBI (no phosphoric acid) (—); (b) PBI/PTFE-2 (38.0 wt% phosphoric acid) (---); (c) PBI/PTFE-2 (no phosphoric acid) (- - ●); (d) PTFE (-●).

ing 38.0 wt% phosphoric acid) [curve (b)] happened due to the continuing dehydration of pyrophosphoric acid to polyphosphoric acid ($\text{H}_4\text{P}_2\text{O}_7 \rightarrow 2\text{HPO}_3 + \text{H}_2\text{O}$) [28]. These curves show the water content of these membranes decreases in the sequence of: PBI > PBI/PTFE (38.0 wt% phosphoric acid) > PBI/PTFE (0.0 wt% phosphoric acid) > PTFE. These results suggest that PBI membrane had largest water content and PTFE membrane had smallest water content in these membranes. The introducing of porous PTFE into PBI decreased the water content of membranes. These data also show that PBI has a better thermal stability than PTFE. Though the introducing of porous PTFE into PBI caused a decrease of thermal degradation temperature. However, the degradation temperature $\sim 350^\circ\text{C}$ for PBI/PTFE composite membranes [curve (b)] is much higher than the working temperature ($\leq 200^\circ\text{C}$) of PEMFC. Thus the thermal stability of PBI/PTFE composite membranes is qualified for PEMFC application.

3.5. Mechanical strength

The tensile strength of PBI/PTFE-2 composite membrane is 73.3 ± 5.8 MPa and that of PBI membrane was 31.2 ± 1.9 MPa. This result shows that the mechanical strength of PBI was improved by reinforcing with a porous PTFE supporting film.

3.6. Single fuel cell performance test

In order to evaluate the fuel cell performance of our composite membranes, PBI and PBI/PTFE-2 composite membranes were used to prepared membrane electrode assemblies (MEA) and the PEMFC single cells performances were tested at 150 and 180°C under H_2 and O_2 flow rates of 100 ml/min. Fig. 7 shows the cell potential V versus current density i curves of single fuel cells prepared from PBI and PBI/PTFE-2 composite

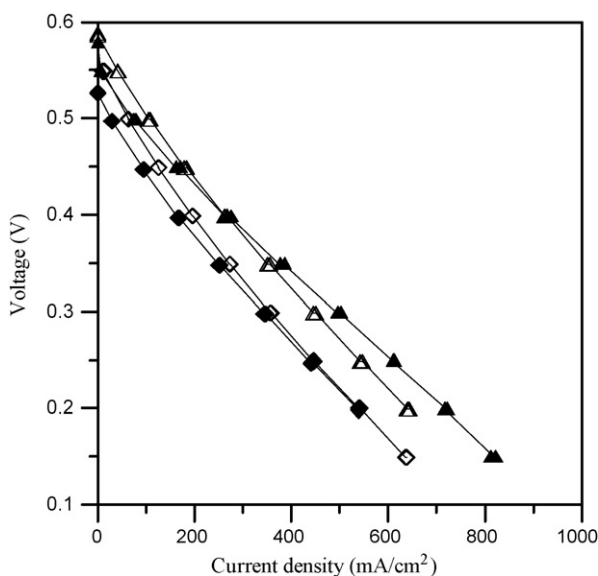


Fig. 7. PEMFC single cell voltage vs. current density of MEA prepared from PBI (100 μm) and PBI/PTFE-2 (22 μm) and operated at various temperatures. (\diamond) PBI at 150°C ; (\triangle) PBI at 180°C ; (\blacklozenge) PBI/PTFE-2 at 150°C ; (\blacktriangle) PBI/PTFE-2 at 180°C .

Table 4
OCV data of PEMFC single cells

	Temperature ($^\circ\text{C}$)	
	150	180
PBI (V)	0.553	0.590
PBI/PTFE-2 (V)	0.532	0.570

membranes. Table 4 summarized PEMFC open circuit voltages of these two PEMFCs operated at 150 and 180°C .

The cell voltage at open circuit, i.e. the open circuit voltage (OCV), usually does not reach the theoretical value of the overall reversible cathode and anode potentials at the given pressure and temperature. One of the reasons of the lowering of OCV from theoretical voltage has been attributed to the penetration of fuel across the membrane [29]. Comparing with the literature reports [2,4], our present OCV data were lower than those reported in literature. The reason for the low OCV values of our present results could be attributed to the poor hardware design of inlets of H_2 and O_2 gas flow channel plates and a small amount of gas leakage occurred during the single cell performance test. We had carried out single cell test using PBI based MEAs, i.e. Celtec-P 1000 MEA, purchased from PEMEAS Fuel Cell Technologies Co. with the same single cell hardware design and obtained an OCV value about 15–20% lower than that reported from PEMEAS Fuel Cell Technologies Co. [30]. After correction with the factor of single cell hardware design, the OCV values of the MEAs in our present work should be around 0.65–0.75 V. However, the main purpose of this work was to compare the PEMFC performances of MEAs prepared from PBI/PTFE-2 (thickness = 22 μm) and pure PBI (thickness = 100 μm) membranes. The poor hardware design would not affect the comparison results between MEAs prepared from PBI/PTFE and pure PBI membranes. Table 4 shows that for a same MEA, the OCV value increased with increasing operating temperature, due to the higher electrochemical reaction rate at a higher temperature. However, at a fixed PEMFC operating temperature, the MEA prepared from PBI/PTFE-2 (thickness 22 μm) had a lower OCV value than that prepared from PBI (thickness 100 μm), indicating a higher penetration of fuel across PBI/PTFE-2 membrane than that of fuel across PBI membrane. The OCV data were quite consistent with gas permeation data shown in Table 2. In Table 2, we found that PBI/PTFE-2 had higher gas permeation than PBI, due to the lower thickness of PBI/PTFE-2 than PBI.

Fig. 7 shows the voltages of single fuel cells fall as current density increases. One of the reasons for the falling down of the voltage with increasing current density is the so called “ohmic loss” which comes from the resistance to the flow of ions through the polymer electrolyte membrane [29]. It is found that though the PBI/PTFE-2 composite membrane has a lower ionic conductivity than PBI membrane, however, owing to the thinner thickness of composite membranes than PBI membranes, the PBI/PTFE-2 has a shorter pathway for transporting proton. Thus MEA prepared from PBI/PTFE-2 composite membrane had a lower slope of voltage against current density while the current

density $i \geq 200 \text{ mA/cm}^2$ and thus a lower “ohmic loss” than PBI membrane. These results were consistent with the “resistance r ” data shown in Table 3.

4. Conclusions

In this work, we show that PFSI resin is an excellent coupling agent for PTFE and poly(benzimidazole) (PBI). Using PFSI as a coupling agent for PBI and porous PTFE, we successfully prepared PBI/PTFE composite membranes. The PBI/PTFE composite membrane had a film thickness of $\sim 22 \mu\text{m}$ and thus a lower proton resistance than a PBI membrane with a film thickness of $\sim 100 \mu\text{m}$. Because of higher mechanical strength of PTFE than PBI, for fuel cells applications, the thickness of PBI/PTFE composite membranes can be made lower than that of PBI membranes. The PEMFC single cell tests showed that PBI/PTFE composite membranes had a better performance than PBI membranes at 180°C , because of the thinness of the PBI/PTFE composite membranes and thus lower resistance of the proton exchange membranes.

Acknowledgement

The authors would like to thank for the financial support by Bureau of Energy, Ministry of Economy Affairs of ROC through grants 94-D0122.

References

- [1] K.V. Kordesch, G.R. Simader, Fuel Cells and Their Applications, VCH Publishers Inc., Weinheim, Germany, 1996, Chapter 4.
- [2] J.S. Wainright, M.H. Litt, R.F. Savinell, in: W. Vielstich, A. Lamm, H.A. Gasteiger (Eds.), Handbook of Fuel Cells, vol. 3, John Wiley & Sons, New York, 2003, Chapter 34.
- [3] H.A. Gasteiger, M.F. Mathias, in: M. Murphy, T.F. Fuller, J.W. Van Zee (Eds.), Proceedings of the Symposium on Proton Conducting Membrane Fuel Cells. Part III, The Electrochemical Society, Pennington, NJ, 2005, PV 2002-31, p. 1.
- [4] M. Rikukawa, K. Sanui, Prog. Polym. Sci. 25 (2000) 1463–1502.
- [5] R.F. Savinell, M.H. Litt, US patent 5,525,436 (1996); 6,025,085 (2000); 6,099,988 (2000).
- [6] K.D. Kreuer, J. Membr. Sci. 185 (2001) 29–39.
- [7] P.D. Genova, J. Membr. Sci. 185 (2001) 59–71.
- [8] Q. Guo, J. Membr. Sci. 154 (1999) 175–181, sulfonated poly(phenoxy phosphazene).
- [9] J.S. Wainright, J.T. Wang, D. Weng, R.F. Savinell, M.H. Litt, J. Electrochem. Soc. 142 (1995) L121–L123.
- [10] J.T. Wang, R.F. Savinell, M.H. Litt, H. Yu, Electrochim. Acta 41 (1996) 193–197.
- [11] R.M. Penner, C.R. Martin, J. Electrochem. Soc. 132 (1985) 514–515.
- [12] C. Liu, C.R. Martin, J. Electrochem. Soc. 137 (1990) 510–515.
- [13] C. Liu, C.R. Martin, J. Electrochem. Soc. 137 (1990) 3114–3120.
- [14] M.W. Verbrugge, R.F. Hill, E.W. Schneider, AIChE J. 38 (1992) 93–100.
- [15] B. Bahar, A.R. Hobson, J. Kolde US Patent 5,547,551 (1996).
- [16] K.M. Nouel, P.S. Fedkiw, Electrochim. Acta 43 (1988) 2381–2387.
- [17] A.E. Steck, C. Stone, US Patent 5,834,523 (1998).
- [18] J.E. Spethmann, J.T. Keating, WO Patent 98/50,457A1 (1998).
- [19] S. Banerjee, J.D. Summers, WO Patent 98/51,733A1 (1998).
- [20] F. Liu, B. Yi, D. Xing, J. Yu, H. Zhang, J. Membr. Sci. 212 (2003) 213–223.
- [21] J. Shim, H.Y. Ha, S.A. Hong, I.H. Oh, J. Power Source 109 (2002) 412–417.
- [22] H.L. Lin, T.L. Yu, K.S. Shen, L.N. Huang, J. Membr. Sci. 237 (2004) 1–7.
- [23] H.L. Lin, T.L. Yu, L.N. Huang, L.C. Chen, K.S. Shen, G.B. Jung, J. Power Sources 150 (2005) 11–19.
- [24] M. Ueda, M. Sato, A. Mochizuki, Macromolecules 18 (1985) 2723–2726.
- [25] E.W. Choe, D.D. Choe, in: J.C. Salamone (Ed.), Polymeric Materials Encyclopedia, CRC Press, Boca Raton, FL, 1996, p. 5619.
- [26] W.G.F. Grot, Nafion Perfluorinated Membranes Product Bulletin–Nafion® as a Separator in Electric Cells, DuPont Polymer Products Department, 1986.
- [27] C. Hasiotis, Q. Li, V. Deimede, J.K. Kallitsis, C.G. Kontoyannis, N.J. Bjerrum, J. Electrochem. Soc. 148 (2001) A513–A519.
- [28] S.R. Samms, S. Wasmus, R.F. Savinell, J. Electrochem Soc. 143 (1996) 1225–1232.
- [29] J. Larminie, A. Dicks, Fuel Cell Systems Explained, John Wiley & Sons Ltd., Chichester, England, 2000, Chapter 3.
- [30] PEMEAS Fuel Cell Technologies website, 2006. www.pemeas.com.